PREDICTION OF ROOM TEMPERATURE MECHANICAL PROPERTIES IN ALUMINIUM CASTINGS

Zhanli GUO, Nigel SAUNDERS, Peter MIODOWNIK, Jean-Philippe SCHILLÉ

Sente Software Ltd., Surrey Technology Centre, Guildford GU2 7YG, U.K.

Keywords: Aluminium alloys, Mechanical properties, Casting alloys, Dendrite arm spacing

Abstract

Prediction of material properties for alloy castings is an old dream of foundrymen and casting designers. As the recent development of JMatPro computer software has made it possible to successfully model physical and thermophysical properties during solidification , it is a natural step to go further and to predict the mechanical properties of casting alloys. The aim of the present work is to develop a model that can be used to calculate the room temperature mechanical properties for a wide range of cast aluminium alloys. The model calculates mechanical properties based on the microstructure in the casting, which is determined by the chemical composition and casting conditions. The first part of the paper describes the microstructural evolution during solidification, where the cooling curve during solidification and dendrite arm spacing (DAS) are calculated as a function of the alloy chemistry and initial cooling rate. The second part features the development of a model for strength calculation. The strengthening mechanisms considered are solid solution strengthening, precipitation hardening and the DAS size effect. The phases that contribute to strengthening includes primary phases, various types of eutectics and intermetallics. Finally a strength-hardness conversion and calculation of the stress-strain curve are provided.

Introduction

Cast aluminium alloys have widespread applications for structural components in the automotive industry. They have been used or demonstrated successfully in power-train applications including engine blocks, cylinder heads, and transmission cases. However, to achieve the maximum impact on fuel efficiency, the application of cast aluminium alloys has to be extended to more critical structural parts, such as brake valves and callipers which are traditionally made of cast iron and steels. The most significant barrier to the acceptance of cast aluminium in many structural applications has been its reputation for variability in mechanical properties. Anything that may help control or predict the results of casting variables would be of great benefit to industry as it eases the reliance on extensive inspection and non-destructive evaluation. It is the aim of this work to develop a physical model to calculate the room temperature mechanical properties of aluminium castings.

Mechanical properties are linked to the microstructure in the material, which is determined by the chemical composition (trace elements and alloying elements) and casting conditions (solidification rate and casting defects). In practice, solidification occurs under non-equilibrium conditions during which the microstructural evolution can be modelled based on the so-called Scheil approach. This approach has proved to yield excellent results for aluminium alloys [1] and will be adopted in the present study to provide the necessary microstructural information for further mechanical property modelling.

Typical casting microstructural features consist of primary phases (dendritic Al phase or primary silicon particles), eutectics (Al-Si, Al-Al_2Cu, Al-Al_3Mg_2 etc.) and intermetallics (AlFeSi,

$Al_5Cu_2Mg_8Si_6$ etc.) formed during solidification. The mechanisms used to describe the strengthening contribution from the various phases present include solid solution strengthening and precipitation hardening [2,3,4]. Whenever appropriate, these models will be applied in the present study. In cases where no well-recognised physical models are available, semi-empirical approaches have been taken to fill in the knowledge gap. The model developed here differs from previous work [3,4,5] in that it can be applied to a wide range of commercial aluminium alloys and the calculations are carried out in an automatic fashion. Directions for future improvement of the model will also be discussed.

Calculation of Microstructural Features

Phase evolution during solidification

The phase evolution in aluminium alloys during casting can be modelled straightforwardly via the Scheil approach [1], which can be carried out using thermodynamic calculations [6]. This calculation provides the necessary information for further property modelling, such as phase fractions and composition. For instance, the information for hypoeutectic Al-Si alloys includes the fractions of primary Al phase and Al-Si eutectic, the percentages of the Al phase and Si in the Al-Si eutectic, and the fractions of other possible intermetallics formed during solidification in the presence of other alloying additions.

The basic assumption for the Scheil approach is that solute diffusion in the solid phase is small enough to be considered negligible and that diffusion in the liquid is extremely fast, fast enough to assume that diffusion is complete. Although a full model for solidification behaviour requires the incorporation of a kinetic analysis of micro-segregation and back diffusion, the predictions of the basic Scheil model have proved to be close to reality for most cast aluminium alloys [1]. The predictions for fraction solid transformed as a function of temperature have been compared with those measured during an extensive experimental programme [7,8,9] which examined the solidification behaviour of almost 40 commercial aluminium alloys. Comparisons for some of these alloys are shown in Fig. 1. The agreement is most striking and the level of accuracy achieved for these alloys is quite typical of that attained overall in the comparison.

Backerud et al. [7,8] also produced detailed studies concerning the phases observed during solidification. For aluminium alloys the number of such phases can be large and their appearance or non-appearance is very dependent on minor impurity levels. The comparison between the phases observed by Backerud et al. and those predicted is very good [1]. Fig. 2 shows the calculated fraction solid vs. temperature for an A356 alloy. The formation and amount of minor phases

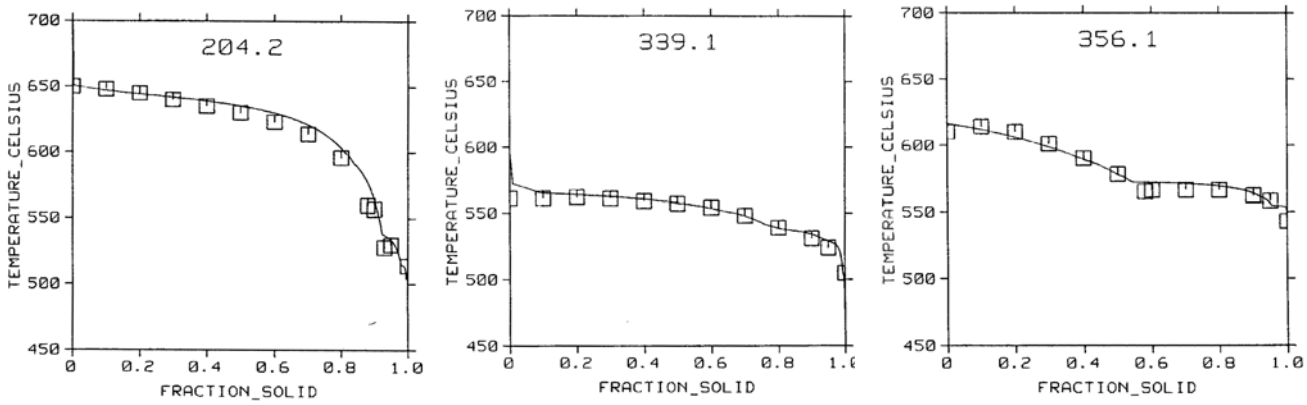

Fig. 1. Fraction solid vs. temperature plots for various cast aluminium alloys calculated under Scheil condition with experimental results (□) of Backerud et al [8] shown for comparison.

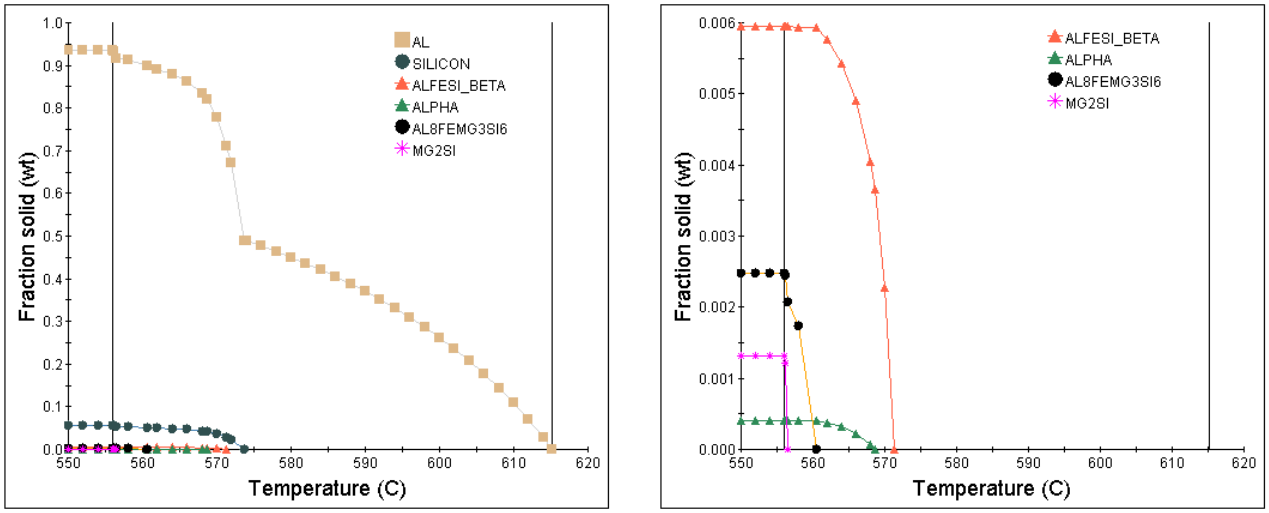

Fig. 2. Calculated fraction solid vs. temperature plot for an A356 alloy, (a) major phases including Al and Si, and (b) minor phases such as AlFeSi and $Al_8FeMg_3Si_6$

including intermetallics AlFeSi and $Al_8FeMg_3Si_6$ are clearly illustrated. The fraction of Al phase at the start of the silicon formation is of dendritic form.

Cooling curve during solidification

A common practice is to estimate the fraction solid curve during solidification from the measured cooling curve [10,11]. This section describes a reverse procedure, i.e., how to calculate the cooling curve during solidification based on the fraction solid curve calculated in the previous section, when the initial cooling rate is given.

During solidification, there are two heat-related processes. One is the release of latent heat due to the progress of the transformation from liquid to solid phases; and the other is the heat extraction from the sample by external media. Different cooling rates reflect different heat extraction abilities of the external media. At the initial stage of cooling before any solid phase forms, normally a constant cooling rate V_c can be maintained. The heat extraction rate Q_{ext} can therefore be calculated as:

$$Q_{ext} = A_1 C_p V_c \quad (1)$$

where A_1 is a material constant that can be cooling rate dependent, and C_p is the specific heat without considering phase transformations. Q_{ext} is assumed not to change during cooling. The total extracted heat after time t can then be calculated as:

$$H_{ext} = Q_{ext} t \quad (2)$$

The latent heat released (H_{rel}) up to a certain temperature can be calculated from the fraction solid formed at that temperature as a fraction of the overall transformation latent heat:

$$H_{rel} = f_s(T) L \quad (3)$$

where $f_s(T)$ is the fraction solid formed when cooling down to temperature T and L is the latent heat of the transformation.

As $H_{rel}(T)=H_{ext}$ always holds during solidification, one can calculate the time required to reach a certain temperature, i.e. the time-temperature cooling curve. It should be noted that there can be a natural decrease in the value of V_c depending on the cooling method. This has been considered in

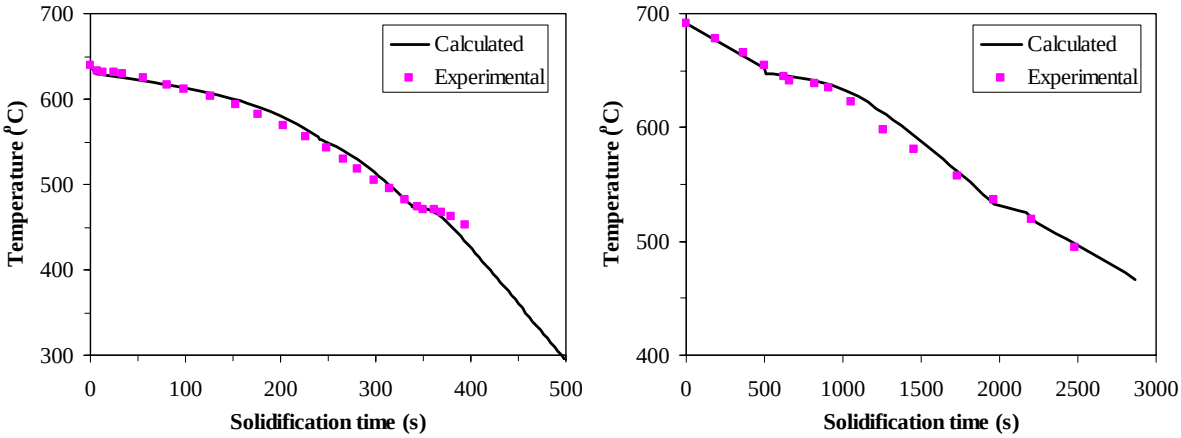

Fig. 3. Comparison between calculated and experimental cooling curves, (a) 7075 alloy at 1.1 °C/s [7], (b) an AlCuSi alloy at 0.08 °C/s [12]

the calculation of cooling curve for aluminium alloys when appropriate. The cooling curves calculated for two aluminium alloys, 7075 and Al-3.7Cu-0.47Si, are shown in Fig. 3, in comparison with experimental curves [7,12].

Dendrite arm spacing calculation

The cooling rate affects the structure of as-cast alloys in a well-established manner, i.e. the dendrite arm spacing (DAS) decreases with increasing cooling rate. Because DAS is one of the important factors that affect the mechanical properties of cast materials, it is of great importance to be able to predict DAS during the early stages of designing a casting process.

Extensive research has been carried out to study the relationship between DAS with cooling rate. This relationship between the velocity of dendrite tip, thermal gradient and DAS has been derived theoretically as: [13]

$$\lambda = A(GR)^{-n} \tag{4}$$

where λ denotes the dendrite arm spacing, G the thermal gradient at the solid-liquid interface, R the velocity of the dendrite tip, A is an alloy-dependent parameter and n is an exponent equal to 1/3. This relationship takes into account the coarsening of dendritic arms during solidification, when finer branches disappear and thicker branches survive.

In industrial practice, it is difficult to measure the velocity of the dendrite tip. Therefore, the above relationship has been validated with respect to the cooling rate (substituting V_c for GR in Eq. 4) and the average dendrite arm spacing [13]:

$$\lambda = AV_c^{-n} \tag{5}$$

Different values for A and n in Eq. 5 are reported in literature for different aluminium alloys [14]. Their values vary greatly even within the same alloying system. Most studies have shown that DAS decreases with increasing concentration of alloying elements [12,15,16], although there are studies reporting no composition effect on DAS [17]. In the present work, it is found that a composition effect has to be considered so as to make the relationship between cooling rate and DAS adequate enough for practical use. A typical form used by some previous researchers, is given in equation (6) [12,16]:

$$\lambda = Ax_i^{m_i} x_j^{m_j} (...)V_c^{-n} \tag{6}$$

where x_i, x_j are the concentrations of influential alloying elements and m_i, m_j the corresponding

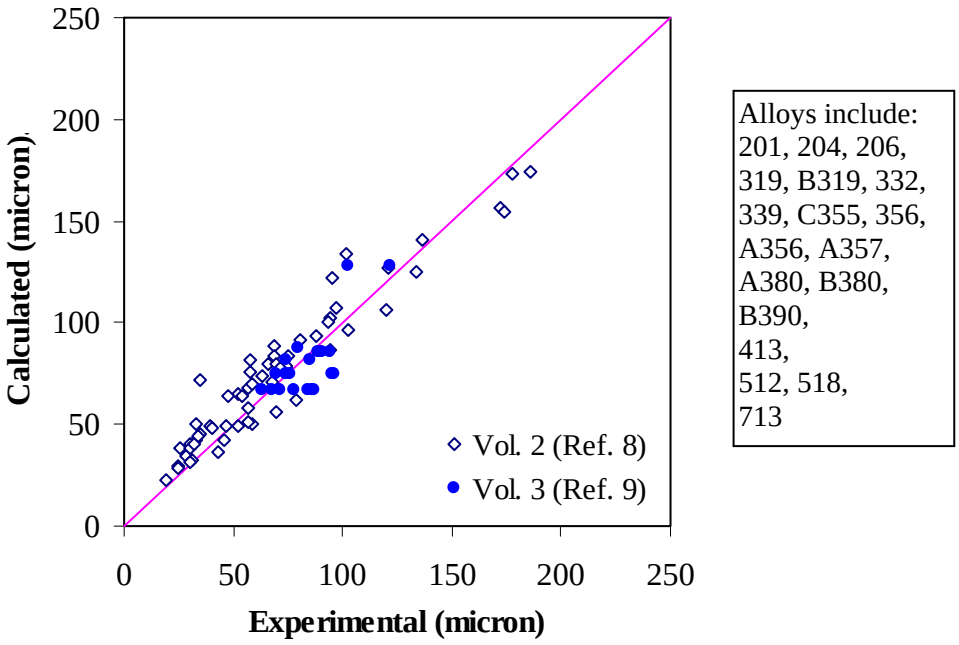

Fig. 4. Comparison between experimental and calculated DAS for a variety of commercial aluminum alloys

concentration exponents. This equation can be useful in some cases, but the fact that the values of m_i and m_j are negative makes it impossible to be applied to systems not containing these elements. So another form of composition dependence has to be used if the equation is to be applicable to a wide range of alloys. The present study makes the material constant A composition dependent in the following form:

$$A = A_0 / (\sum_i c_i x_i + \sum_{i,j} c_{ij} x_i x_j) \tag{7}$$

where c_i, c_{ij} are the corresponding coefficients and A_0 is a constant independent of alloy chemistry. Combining Eqs. 5 and 7, one has

$$\lambda = A_0 / (\sum_i c_i x_i + \sum_{i,j} c_{ij} x_i x_j) V_c^{-n} \tag{8}$$

The values for these coefficients are empirically fitted against experimental data [8,9]. Comparison between calculation and experimental data is shown in Fig. 4, which covers a wide range of cast aluminium alloys and a wide range of cooling rates.

There are various of ways to define the cooling rate of a solidification process. (a) It can be the average cooling rate, i.e. the solidification temperature interval (liquidus minus solidus) divided by the time required to complete solidification; or (b) it can be defined as the rate of heat extraction from the solidifying volume, i.e. the so-called tip cooling rate; or (c) it can be the slope of the cooling curve at a specific temperature (usually either liquidus or solidus). On the one hand, the cooling rate to be used should reflect the dendrite formation process, otherwise Eq. 8 would be of little physical meaning. On the other hand, the necessary parameters should be capable of measurement and control, otherwise Eq. 8 would be of no practical use. In this respect, the average cooling rate and tip cooling rate are not really suitable for use as they are uncontrollable. The cooling rate is affected by the release of latent heat and changes continuously during solidification but is generally quite constant above the liquidus before the start of solidification, where it reflects the ability of heat extraction of the cooling media and where it is also possible for it to be controlled. Therefore, the cooling rate used in the present study takes this definition.

Strength Calculation

Based on the microstructural information calculated in the previous section, the next step is to quantify the contribution from each constituent to mechanical properties. Typical contributions to the strength of cast aluminium includes solid solution strengthening and precipitation hardening due to intermetallics. The properties to be calculated are yield strength, tensile strength, and the stress-strain curve. The yield strength is calculated in this section using the Al-Si system as an example and other properties in the next section. Al-Si alloys usually contain 5-20% Si (in wt% unless stated otherwise). The microstructural features of these alloys consist of a primary phase, either aluminium dendrites (hypoeutectic) or silicon particles (hypereutectic), and a eutectic mixture of these two phases. There may also be other intermetallic phases formed during solidification, depending the addition of other alloying elements.

Primary phases

The strength contribution from primary silicon particles can be considered negligible due to their large size [18,19]. Special processing techniques can produce finer primary silicon particles so as to achieve better ductility and the strengthening can then be modelled according to Orowan's looping mechanism for dispersion strengthening [19].

The main focus here is therefore to calculate the strength contribution from the dendritic structure of the primary Al phase. First solid solution strengthening is calculated, and then the size effect of DAS on strength will be added. The methodology adopted for solid solution strengthening of one phase is described by the following equation:

$$\sigma_0 = \sum_i x_i \sigma_i^o + \sum_i \sum_j x_i x_j \Omega_{ij} + \ldots \quad (9)$$

where σ_0 is the total strength, σ_i^0 is the strength of pure element i, x_i and x_j are the atomic fractions of elements i and j, and the values of Ω_{ij} are associated with the solute interactions obtained based on information from Ref. 20. It should be noted that other sources have reported strengthening coefficients of significantly different values. For instance, Court et al. [21] claimed that the effect of Mn on the yield stress is 115 MPa/wt%, while 30.3 MPa/wt% is reported by Ref. 20. However, as the solubility of Mn in Al is very small, such difference in strengthening coefficient would not cause much difference in the overall alloy strength. As an example, Fig. 5 shows the calculated Cu effect on the yield strength of aluminium alloys, in comparison with experimental data. As the amount of Cu in Al is usually up to 5 wt%, the discrepancy at concentrations higher than that would not affect the present calculation

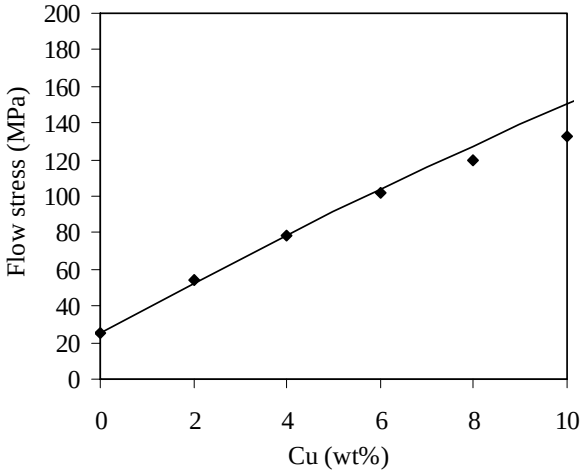

Fig. 5. The calculated Cu effect on yield strength of aluminium alloys, in comparison with experimental data

The Hall-Petch equation is used to describe the strength variation due to change in DAS size:

$$\sigma_{den} = \sigma_0 + k_{den} \lambda^{-0.5} \quad (10)$$

where σ_{den} and k_{den} are the flow stress and the Hall-Petch coefficient for the dendritic phase. As the grain size in the as-cast condition is usually very large for aluminium alloys, its effect on strength is not considered in the present study. Different values of k_{den} have been reported for different alloys [5,22,23]. However, the values reported may not be appropriate if not all the strengthening mechanisms were considered when estimating k_{den}. In the present study, k_{den} is set as a constant value 0.25 MPa.m$^{-1/2}$ for simplification.

Strength of the eutectic structure

The strength of the eutectic structure consists of a contribution from the two co-precipitating phases Al and Si, as well as the possible strengthening due to the silicon particles. The particle size is affected by the cooling rate and can be fibrous or platelike. The eutectic strength is a function of the fibrosity of these particles in that a fibrous structure leads to higher resistance to yielding [24,25]. The fineness of the eutectic microstructure is closely related to the size of DAS. As there is no standard model available to describe the contribution from the size/morphology on strength of the eutectic, a formula based on the Hall-Petch relationship has been employed. The strength of the Al-Si eutectic is then given by:

$$\sigma_{eut} = \left(f_{Al}\sigma_{Al} + f_{Si}\sigma_{Si} \right) / \, f_{eut} + k_{eut}\lambda^{-0.5} \tag{11}$$

where f_{Al} and f_{Si} and are the fractions of Al, Si in the Al-Si eutectic, respectively, and σ_{Al} and σ_{Si} the strength of Al, Si in the Al-Si eutectic. σ_{Al} is effectively the σ_o in Eq. 9 and σ_{Si} is set as a constant. f_{eut} is the fraction of the eutectic ($f_{eut} = f_{Al} + f_{Si}$), and k_{eut} the Hall-Petch coefficient.

Such a treatment reflects the observed effect of the cooling rate on the strength of the eutectic, in that faster cooling results in a finer eutectic and in turn higher strength. The Hall-Petch coefficient is obtained through fitting against experimental data for alloys Al-6.5Si [26], Al-7Si and Al-12.6Si [27] where no interference from intermetallics or the dendritic Al phase exists.

Precipitation strengthening due to intermetallics

Many types of intermetallics may form during solidification. Their contribution to strength can be described by theories for precipitation strengthening [28,29,30]. In the present study, these precipitates are assumed to be unshearable and their contribution to strength is modelled via the Orowan looping mechanism as used by previous researchers [31]. This mechanism was first proposed by Orowan [32], and later further developed by Ashby [33] to take into account the effects of a statistical distribution of particle spacings. The Ashby-Orowan relationship is given as

$$\sigma_{ppt} = 0.84M\left(\frac{1.2Gb}{2\pi L}\right)\ln\frac{r}{b} \tag{12}$$

where σ_{ppt} is the strength contribution from precipitates, and M is the Taylor factor (normally a value close to 3). r is the particle radius, b the burger's vector, G the shear modulus, and L the inter-particle spacing. Assuming the precipitates are spherical, the relationship between precipitate fraction f_{ppt}, inter-particle spacing L and particle radius r is given by [34]:

$$L = \left(1.23\sqrt{\frac{2\pi}{3f_{ppt}}} - 2\sqrt{\frac{2}{3}} \right) r \tag{13}$$

It is difficult to estimate the particle size formed during solidification. However, the change in size follows a coarsening law, and can therefore be assumed to be proportional to $t^{1/3}$ [35,36,37]. As time t is inversely proportional to the cooling rate, it is reasonable to assume the particle size to be proportional to $V_c^{-1/3}$.

$$r = r_0 * V_c^{-1/3} \tag{14}$$

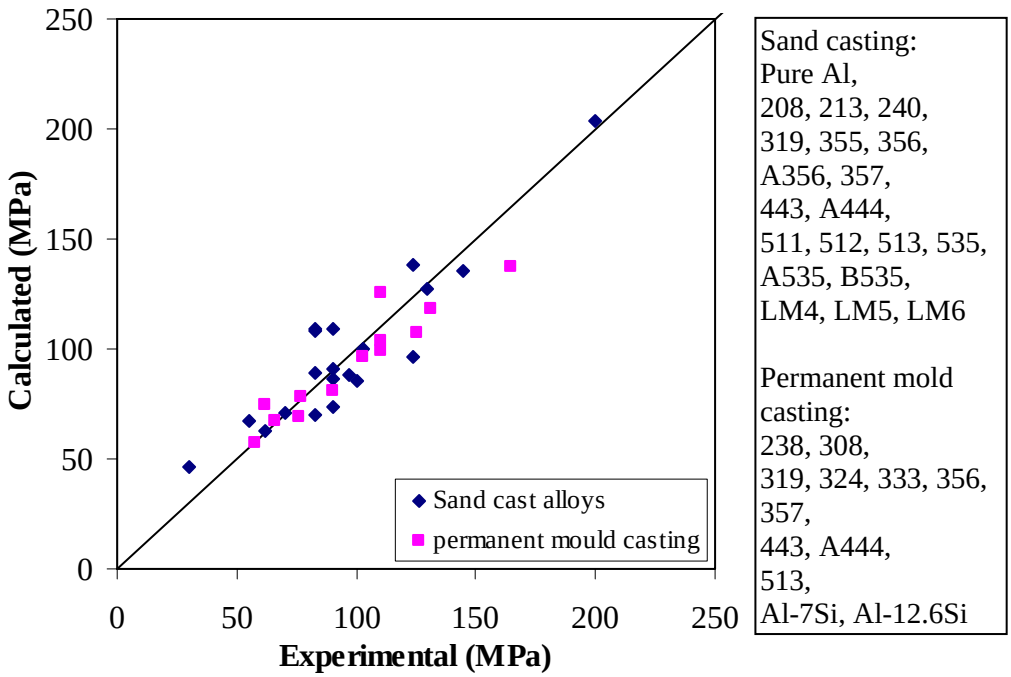

Fig. 6. Comparison between experimental and calculated yield strength of various alloys from sand casting and permanent mold casting.

where r_0 is a constant, independent of alloy chemistry, obtained by fitting against experimental data. This assumption is supported by experimental observations [38,39], though the value of the exponent is not exactly equal to -1/3. It is possible to calculate the strength contribution from each precipitate type individually, but to simplify the situation, all the precipitates were considered as one group of the same size.

Calculation of overall strength and validation

The eutectics formed in aluminium alloys can be of types other than Al-Si, such as Al-Al_2Cu and Al-Al_3Mg_2. Their strength can be modelled using equations similar to Eq. 11. The overall yield strength of an casting alloy can be calculated as

$$\sigma_y = f_p\sigma_p + \sum_i f_i\sigma_i + \sigma_{ppt} \qquad (15)$$

where f_p and σ_p are the fraction and strength of the primary phase, i.e. the dendritic phase in this study, and f_i and σ_i correspond to various types of eutectics, respectively.

The model developed has been tested extensively against experimental data and a comparison plot is shown in Fig. 6, where each data point represents one commercial alloy, either from sand casting or permanent mold casting. It can be seen that it covers all types of cast aluminium alloys except the 7xx series (Al-Mg-Zn alloys). The 7xx series differ from other types in that elementary Zn may precipitate out of solid solution at temperatures below 200°C, which may harden the alloy. The cooling rates for sand casting and permanent mold casting are 0.3°C/s and 0.65°C/s, respectively.

Strength-hardness Conversion and Stress-strain Curves

The model described in the previous section allows the calculation of the yield stress. It would also be very useful to know other mechanical properties such as tensile stress and hardness. Quantitative relationships between these properties were developed by Tabor [40] based on the assumption that stress σ is related to strain ε via work-hardening coefficient m and constant B:

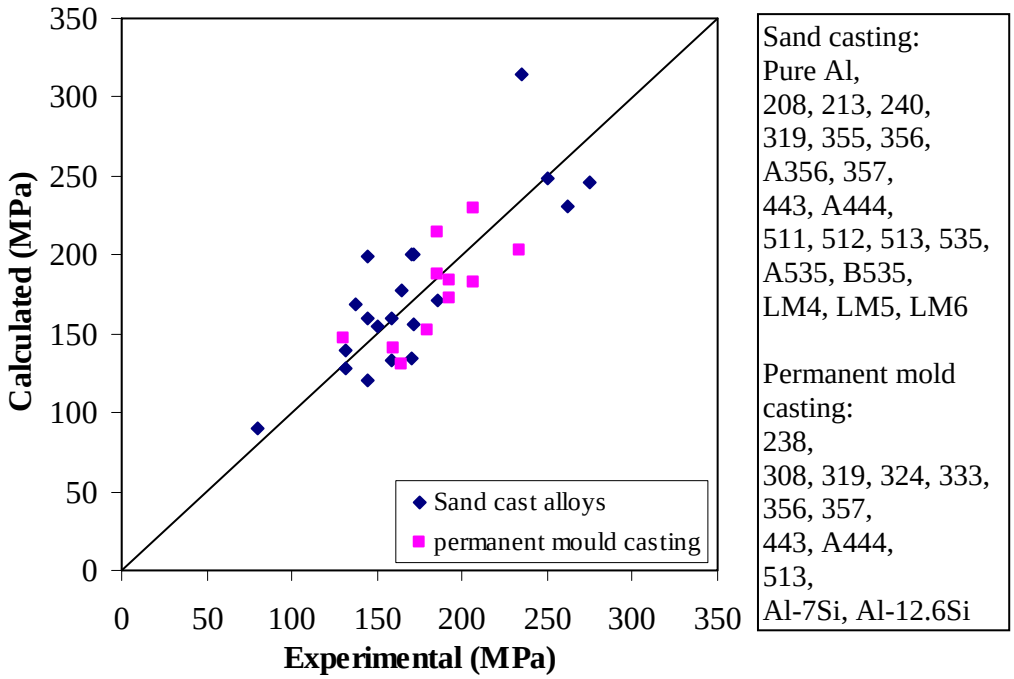

Fig. 7. Comparison between experimental and calculated tensile strength of various alloys from sand casting and permanent mold casting.

$$\sigma = B\varepsilon^{m} \tag{16}$$

By determining the average pressure under a hardness indenter of a given geometry, it is possible to derive equations for the relationships among hardness, yield stress σ_y and tensile stress σ_t:

$$Hv = C\sigma_y (40)^{m} \tag{17}$$

$$\sigma_t = \sigma_y (40)^{m} (1-m)\left(\frac{12.5m}{1-m}\right)^{m} \tag{18}$$

where C lies between 2.9 and 3.3, which is in good agreement with a theoretical value of 3; and related to the yield stress according to the relationship:

$$m = a\exp(b\sigma_y) \tag{19}$$

where a and b are alloy dependent and their values are fitted empirically. The tensile strength was then calculated based on the yield strength calculated for cast aluminium alloys, Fig. 7. Good agreement between calculations and experimental data was obtained again for a wide range of casting alloys.

For most of the alloys, the stress-strain curve can be considered as the sum of an elastic region and a plastic region. In the elastic region, the stress is proportional to the strain according to Hooke's law. In the plastic region, the stress is related to strain via Eq. 16. To calculate a stress-strain curve, the input parameters required are then only Young′s modulus and either yield strength, or tensile strength, or even just hardness values. Typical stress-strain curves for two Al-Si alloys are shown in Fig. 8, with experimental data from Ref. 27.

Discussion and Future Developments

The model presented here is useful not only because it can help estimate the strength of casting alloys to a useful accuracy, but more importantly, because it is a useful tool for tailoring mechanical properties through the correct choice of chemical composition and casting parameters. It can also

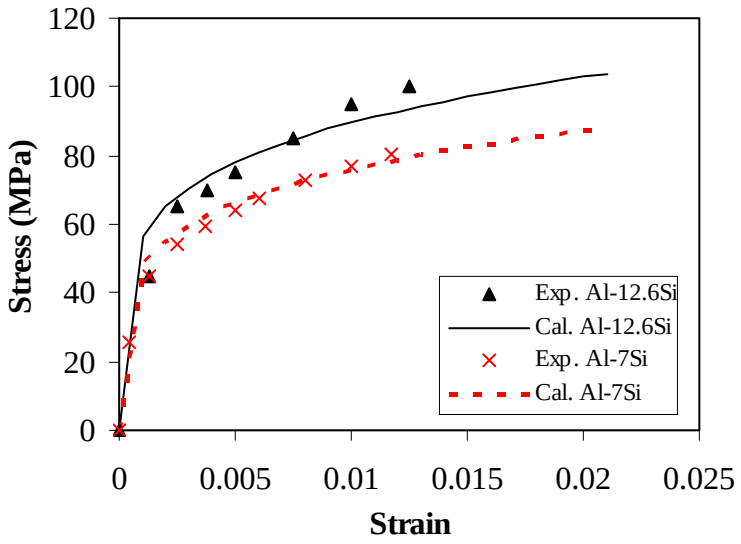

Fig. 8: Comparison between experimental and calculated stress-strain curves for two Al-Si alloys

be used to help analyse the consequences of unintended processing or property variations, and identification of potential improvements.

It is worth mentioning the effect of casting defects on mechanical properties. Strength is affected by casting defects, which in turn depends on casting methods. Sand casting and permanent mold casting generally produce sound quality and the effect of defects such as porosity on strength in these castings can be neglected. The present model can therefore be directly applied to alloys cast by these methods. Die casting, however, tends to trap air during solidification, which gives rise to appreciable amounts of porosity in the casting. As a result, the strength of die castings is usually lower than that of permanent mold castings. Many efforts have been made to understand the detrimental effect of porosity on the tensile properties of aluminium alloys and empirical relationships between the drop in strength and the percentage of porosity have been suggested [41]. By combining the present model's strength calculation and those empirical relationships, it should be possible to also estimate the strength of die castings in future investigation.

Summary

A model has been developed for the calculation of tensile properties in cast aluminium alloys. The model can be applied to a wide range of casting aluminium alloys and casting methods. With only chemical composition and cooling rate as inputs, the model calculates microstructural constituents, cooling curve, dendrite arm spacing and tensile properties, including yield strength, tensile strength and the stress-strain curve for a wide range of aluminium castings. The strengthening mechanisms considered are solid solution strengthening, precipitation hardening and the DAS size effect. The phases that contributes to strengthening includes primary phases, various types of eutectics and intermetallics. The model should be a useful tool for tailoring mechanical properties by correct choice of chemical composition and casting parameters. It can also be used to help analyse the consequences of unintended processing or property variations, and identify potential improvements.

REFERENCES

1. N. Saunders, in *Solidification Processing 1997*, eds. J. Beech and H. Jones, University of Sheffield, Sheffield, 1997, 362-366.

2. H.R. Shercliff, M.F. Ashby, A process model for age hardening of aluminium alloys – I: The model, Acta Metall. Mater., 38(1990) 1789-1802.
3. S.C. Weakley-Bollin, W. Donlon, C. Wolverton, J.W. Jones, and J.E. Allison, Modeling the age-hardening behavior of Al-Si-Cu alloys, Metallurgical and Materials Transactions A, 35A (2004) 2407-2418.
4. M.J. Starink, S.C. Wang, A model for the yield strength of overaged Al-Zn-Mg-Cu alloys, Acta Materialia 51 (2003) 5131–5150
5. S. Brusethaug, Y. Langsrud, Aluminum properties, a model for calculating mechanical properties in AlSiMgFe-foundry alloys, Metallurgical Science and Technology, 18(1)(2000), 3-7
6. N. Saunders and A.P. Miodownik, *CALPHAD – Calculation of Phase Diagrams*, *Pergamon Materials Series vol.1*, ed. R.W. Cahn, (Oxford: Elsevier Science, 1998).
7. L.Backerud, E.Krol and J.Tamminen, Solidification Characteristics of Aluminium Alloys, vol. 1: Wrought Alloys, Tangen Trykk A/S, Oslo, 1986
8. L. Backerud, G. Chai, L. Arnberg, Solidification Characteristics of Aluminum Alloys, vol. 2: Foundry Alloys, American Foundrymen's Society, Des Plaines, USA, 1996.
9. L. Arnberg, L. Backerud, G. Chai, Solidification Characteristics of Aluminum Alloys, Dendrite Coherency, vol. 3, American Foundrymen's Society, Des Plaines, USA, 1996.
10. Jernkontoret Corporation, A Guide to the Solidification of Steels, Stockholm, Sweden, 1977, 12-14.
11. S. Thompson, S.L. Cockcroft and M.A. Wells, Effect of cooling rate on solidification characteristics of aluminium alloy AA 5182, Materials Science and Technology, 20 (2004) 497-504
12. V. Rontó, A. Roósz, The effect of cooling rate and composition on the secondary dendrite arm spacing during solidification, Part I: Al-Cu-Si alloys, Int. J. Cast Met. Res. 13 (2001) 337–342.
13. M.C. Flemings, Solidification Processing, McGraw-Hill, NY, USA, 1974.
14. D. Eskin, Q. Du, D. Ruvalcaba, L. Katgerman, Experimental study of structure formation in binary Al–Cu alloys at different cooling rates, Materials Science and Engineering A 405 (2005) 1–10
15. Y.L. Liu, S.B. Kang, Mater. Sci. Technol. 13 (1997) 331–336.
16. V. Rontó, A. Roósz, The effect of the cooling rate or local solidification time and composition on the secondary dendrite arm spacing during solidification, Part II: Al-Mg-Si alloys, Int. J. Cast Met. Res. 14 (2001) 131–135.
17. J.E. Spinelli, D.M. Rosa, I.L. Ferreira, A. Garcia, Mater. Sci. Eng. A 383 (2004) 271–282.
18. V.C. Srivastava, R.K. Mandal, S.N. Ojha, Microstructure and mechanical properties of Al–Si alloys produced by spray forming process, Materials Science and Engineering A304–306 (2001) 555–558
19. K. Matsuura, K. Suzuki, T. Ohmi, M. Kudoh, H. Kinoshita, H. Takahashi, Dispersion strengthening in a hypereutectic Al-Si alloy prepared by extrusion of rapidly solidified powder, Metallurgical and Materials Transactions A, 35A (2004) 333-339.
20. Metals Handbook, Tenth Edition, Vol. 2, ASM International, 1990, 37-39.
21. S.A. Court, K.M. Gatenby, D.J. Lloyd, Factors affecting the strength and formability of alloys based on Al–3 wt.% Mg, Materials Science and Engineering A319–321 (2001) 443–447.
22. G. Costanza, F. Quadrini, M.E. Tata, Pressure effect on Al alloy cast behaviour: microstructures and mechanical properties, Int. J. Materials and Product Technology, 20(5-6) (2004) 345-357
23. M. Wierzbinska, J. Sieniawski, Effect of dendrite arm spacing on cleavage fracture toughness of Al-5Si-1Cu alloy, International Journal of Cast Metals Research, 17(5) (2004) 267-270.
24. M.F. Hafiz, T. Kobayashi, A study on the microstructure-fracture behaviour relations in Al-Si Casting Alloys, Scripta Metallurgica et. Materalia, 30 (1994) 475-480.

25. J. Paul, H.E. Eckart, Microstructure and mechanical properties of the age-hardening eutectic aluminium-silicon alloy G-AlSi12(CuMgNi), Z. Metallkde. BD.81 (1990), H.11, 816-825.
26. V.C. Srivastava, R.K. Mandal, S.N. Ojha, Microstructure and mechanical properties of Al-Si alloys produced by spray forming process, Materials Science and Engineering A, A304-306 (2001) 555-558.
27. L. Qian, H. Toda, S. Nishido, T. Akahori, M. Niinomi, T. Kobayshi, Numerical simulation of fracture of model Al-Si alloys, Metallurgical and Materials Transactions A, 36A (2005) 2979-2992.
28. T. Gladman, Precipitation hardening in metals, Materials Science and Technology, 15 (1999) January, 30-36.
29. Z. Guo, W. Sha, Quantification of precipitation hardening and evolution of precipitate, Materials Transactions, 43(6) (2002) 1273-1282.
30. K.L. Kendig, D.B. Miracle, Strengthening mechanisms of an Al-Mg-Sc-Zr alloy, Acta Materialia 50 (2002) 4165-4175.
31. G. Liu, G.J. Zhang, X.D. Ding, J. Sun, K.H. Chen, Modeling the strengthening response to aging process of heattreatable aluminum alloys containing plate/disc- or rod/needle-shaped precipitates, Materials Science and Engineering A344 (2003) 113-124.
32. E. Orowan, Internal Stress in Metals and Alloys, The Institute of Metals, London, 1948, p451.
33. M.F. Ashby, in Oxide Dispersion Strengthening, (Eds. G.S. Ansell, T.D. Cooper, F.V. Lenel), Gordon and Breach, New York, 1958, 143-205.
34. J.W. Martin, Precipitation Hardening,2nd Ed., Butterworth-Heinemann, Oxford, 2nd Ed., 1998, pp58-59, 81
35. I.M. Lifshitz, V.V. Slyozov, Journal of Physics and Chemistry Solids, Vol.19, 1961, pp35-50
36. C. Wagner, Z. Elektrochem., Vol.65, 1961, p581.
37. J.W. Martin, R.D. Doherty, B. Cantor (Eds.), Stability of Microstructure in Metallic Systems, 2nd Ed., University Press, Cambridge, 1997, p248, 256.
38. B. Dutta, M. Rettenmayr, Effect of cooling rate on the solidification behaviour of Al-Fe-Si alloys, Materials Science and Engineering, A283 (2000) 218-224.
39. R.C. Dorward, A dynamic quench model for strength predictions in heat-treatable aluminum alloys, Journal of Materials Processing Technoly, 66(1997) 25-29.
40. D. Tabor, “The Hardness of Metals” Ed W.Jackson, H.Frohlich, and N.F.Mott, Oxford University Press, Ch V-VII, 67-114 (1951).
41. G.W. Mugica, D.O. Tovio, J.C. Cuyas, A.C. Gonzalez, Effect of porosity on the tensile properties of low ductility aluminum alloys, Materials Research, 7(2)(2004) 221-229.